BIOMICROFLUIDICS **8**, 064124 (2014)

Microfluidic impedance cytometry of tumour cells in blood

Daniel Spencer, Veronica Hollis, and Hywel Morgan
Faculty of Physical Sciences and Engineering, Institute for Life Sciences, University of Southampton SO17 1BJ, United Kingdom

(Received 22 September 2014; accepted 5 December 2014; published online 12 December 2014)

The dielectric properties of tumour cells are known to differ from normal blood cells, and this difference can be exploited for label-free separation of cells. Conventional measurement techniques are slow and cannot identify rare circulating tumour cells (CTCs) in a realistic timeframe. We use high throughput single cell microfluidic impedance cytometry to measure the dielectric properties of the MCF7 tumour cell line (representative of CTCs), both as pure populations and mixed with whole blood. The data show that the MCF7 cells have a large membrane capacitance and size, enabling clear discrimination from all other leukocytes. Impedance analysis is used to follow changes in cell viability when cells are kept in suspension, a process which can be understood from modelling time-dependent changes in the dielectric properties (predominantly membrane conductivity) of the cells. Impedance cytometry is used to enumerate low numbers of MCF7 cells spiked into whole blood. Chemical lysis is commonly used to remove the abundant erythrocytes, and it is shown that this process does not alter the MCF7 cell count or change their dielectric properties. Combining impedance cytometry with magnetic bead based antibody enrichment enables MCF7 cells to be detected down to 100 MCF7 cells in 1 ml whole blood, a log 3.5 enrichment and a mean recovery of 92%. Microfluidic impedance cytometry could be easily integrated within complex cell separation systems for identification and enumeration of specific cell types, providing a fast in-line single cell characterisation method. [http://dx.doi.org/10.1063/1.4904405]

I. INTRODUCTION

There is a great interest in exploring physical "label-free" markers for the identification of circulating tumour cells (CTCs) with a view to separating these cells from blood. Examples of such markers include size,[1] density,[2] deformability,[3] and dielectric properties.[4]

It has been known for many years that the dielectric properties of tumour cells differ from normal peripheral blood mononuclear cells.[5,6] The tumour cells have a large membrane surface area that is characterised by features such as folds and microvilli. This translates into a larger membrane capacitance when compared with a similarly sized cell that has a smooth membrane. Gascoyne *et al*.[6] measured the dielectric properties of the entire NCI60 panel of tumour cell lines, representative of a wide range of cancer cells and showed that the membrane capacitance of these cells varies across a wide range but is consistently larger than normal leukocytes. As a solid tumour progresses and metastasises, it moves from a well ordered structure to a more disorganised form, and this leads to a change in cell morphology, see Gascoyne and Shim[4] for a review. The normal close contacts between cells are lost due to degradation of the inter-cellular adhesion complexes. Certain cells develop filopodia which leads to enhanced motility allowing them to move into the circulation, thus becoming CTCs. This process is reflected in a change in the cell membrane morphology which increases the specific membrane capacitance.

Dielectrophoresis (DEP) exploits differences in the dielectric properties and size of cells for separation.[7] Early work[5] demonstrated that tumour cells could be separated from normal cells by DEP in batch mode. Over the ensuing two decades many different DEP separation technologies have been developed for isolation and separation of cells. Of particular interest for

CTC isolation is the development of continuous flow processes based on combining DEP with hydrodynamic and sedimentation forces,[8–10] a so called DEP Field Flow Fractionation (FFF) technology.

The DEP separation criteria are dictated by the unique dielectric properties of the cells. These cell characteristics are usually measured using AC electrokinetic techniques, normally a combination of electrorotation and dielectrophoretic cross-over methods.[11] These techniques are very slow (one cell per minute), although batch processing methods have been developed. For example, image processing has been used to measure the DEP crossover properties of hundreds of cells in a single experiment.[12] A higher throughput dielectrophoretic spring method was recently developed to characterise the DEP properties of thousands of cells in a continuous flow at a rate of 10 cells per second.[13] Importantly, AC electrokinetic analysis of cells require re-suspension of cells in a low conductivity buffer, which although osmotically matched can cause ion leakage from the cytoplasm leading to gradual changes in cell properties during the time of analysis.[4]

Microfluidic impedance cytometry (MIC) also measures the dielectric properties of single cells, but at high throughput (up to 1000 cells per second) and does not require re-suspension of cells in low-conductivity buffer; measurements are performed in physiological medium. The technique measures the electrical impedance of single cells as they flow between pairs of microelectrodes fabricated within a microfluidic channel. The simultaneous application of several different measurement frequencies can be used to analyse cells and to discriminate between different cell types.[14,15] Impedance cytometry can be used to differentiate many different cell types, for example, the three main populations of human leukocytes,[16,17] stem cells,[18] or parasite infected cells.[19] Recently, Choi *et al.*[20] developed a DC microfluidic impedance cytometer which can identify cancer cells directly in whole blood without dilution. Using samples spiked with ovarian cancer cells, the detection efficiency was 88%. CTCs were detected in all 24 samples from breast cancer patients and none were found in samples from healthy patients. The detection method relies on the volume difference between packed red blood cells and larger single cells; however, there is a significant variation in the impedance signal for monodisperse beads which is probably due to coincidence. Consequently, the trigger level was set relatively high, so that some of the smaller Her2 positive cancer cells were missed in the clinical samples.

In this paper, we use MIC to measure the dielectric properties of the immortal cell line MCF7, both singly and mixed with whole blood. The MCF7 cell line was isolated from a breast cancer and is commonly used to represent CTCs. These cells also express the epithelial cell marker protein (EpCAM) that enables them to be identified using fluorescent antibodies. They have a large membrane capacitance which dominates their electrical behaviour enabling clear discrimination from leukocytes. Whole blood is often processed to remove erythrocytes by chemical lysis, and it is shown that this procedure does not affect the MCF7 cells. MCF7 cells spiked into whole blood can be discriminated by MIC down to a ratio of 1 per 1000 leukocytes. Lower MCF7 numbers (100 MCF7 in 1 ml whole blood) were measured by combining MIC with magnetic activated cell sorting (MACS). The results demonstrate that the properties of the MCF7 cells measured by MIC are similar to those measured by traditional techniques (DEP). The simplicity of impedance cytometry means that the method could also be integrated within a complex DEP-FFF separation system for identification and enumeration of specific cell types, providing a fast in-line single cell characterisation method.

II. METHODS AND MATERIALS

A. Experimental setup

Microfluidic impedance chips were fabricated as described previously.[16] The chips are made from glass with channels defined in SU8. Platinum electrodes (30 μm wide) were lithographically patterned onto glass substrates. Channels (cross sectional 30 μm $\times$ 40 μm) were made from SU8 and wafers were thermo-compression bonded. Individual chips were diced from bonded wafers. Fluidic inlet and outlet holes were drilled using a desktop CO_2 laser. Chips were clamped onto a plastic 3D printed holder for fluidic and electrical connections. The holder was mounted on an

x–*y*–*z* stage on an optical bench that had capability for simultaneous measurement of single cell fluorescence. All samples were pumped through the chip at 40 μl min^{-1} using a syringe pump (Harvard instruments). Chips were cleaned with 1 ml DI water, 10% bleach and primed with phosphate buffered saline (PBS) supplemented with 2mM EDTA and 0.5% BSA (bovine serum albumin) between each experiment.

The measurement system has been described previously.[21] Briefly, sinusoidal voltages at fixed frequencies were applied to the top electrodes (Fig. 1). Impedance scatter plots were measured using two simultaneous frequencies (0.5 MHz and either 2 or 4 MHz at 2.5 Vpp). The difference in current flowing into the bottom two electrodes was measured using a transimpedance amplifier and digital impedance analyser (Zurich Instruments). Custom software written in Matlab was used for data analysis, including data normalisation and population gating. Cells were also measured with a FACSAria (Becton Dickson) flow cytometer, equipped with two lasers: 488 nm solid state (20 mW, Coherent Sapphire) and 633 nm HeNe (20 mW, JDS Uniphase). FACSFlow sheath fluid (Becton Dickson) was used and sample flow was at a pressure of 70 psi through a 70 mm nozzle. The instrument was controlled by a PC running FACSDiVa software (Becton Dickson).

B. Cell culture

MCF7 cells were grown in 75 cm^2 flasks in 10 ml DMEM (Dulbecco's Modified Eagle Medium) supplemented with 10% (v/v) heat-inactivated FBS (fetal bovine serum), 2 mM L-glutamine, 1 mM sodium pyruvate, 1% NEAA (non-essential amino acids) and penicillin-streptomycin, at 37 °C in 5% CO_2. Cells were detached with trypsin/EDTA, washed and re-suspended in growth medium prior to experiments. In some experiments, the cells were labelled with EpCAM-FITC antibody (Miltenyi Biotec) by adding 50 μl of antibody to 10 μl of stock cell solution (5×10^6 cells/ml) at 5 °C for 10 min, as specified by the manufacturer.

C. Blood sample collection and preparation

Ethical approval was given by the Isle of Wight, Portsmouth and South East Hampshire Local Research Ethics Committee and written informed consent was obtained from all participants. Venous samples were drawn from the antecubital fossa of the elbow into 3.5 ml Vacutainer tubes (Becton Dickinson, Oxon UK) with EDTA-K_3 for anticoagulation. Following collection, the blood tubes were placed on a roller and continually mixed at room temperature;

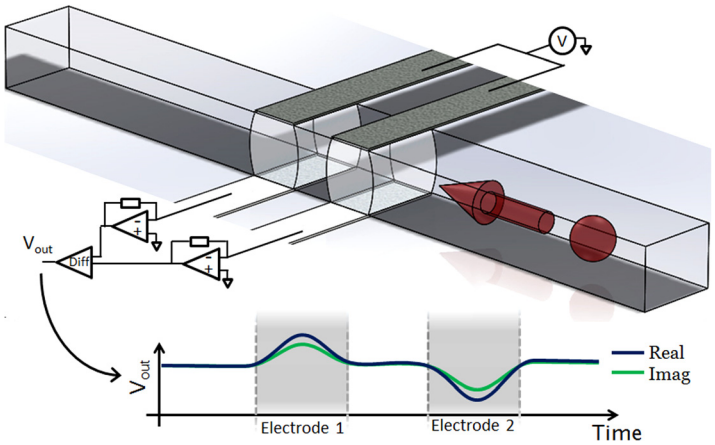

FIG. 1. Illustration showing the structure and operation of the impedance cytometer. The device consists of two sets of parallel facing electrodes (30 μm wide separated by 50 μm) fabricated inside a microfluidic channel (40 μm wide and 30 μm high). Cells suspended in an electrolyte are driven through the channel by pressure driven flow. An AC voltage is applied to the top two electrodes and the difference in current flowing through the bottom two electrodes is measured using a custom detection circuit. Also shown is the idealised differential signal seen when a particle passes through the centre of the device.

all subsequent processing and experimental work was carried out within 6 h. Erythrocytes lysis was performed by addition of lysis solution (0.12% formic acid and 0.05% saponin) to whole blood (12 μl solution per 1 μl blood) with agitation. The reaction was quenched after 6 s by the addition of 0.6% w/v sodium carbonate and 3% sodium chloride, 5.3 μl per μl blood.

D. Magnetic activated cell sorting

To demonstrate enumeration of MCF7 cells by impedance at very low concentrations, cells were first pre-concentrated using a simple MACS method. Proof of principle experiments were performed by adding 10 μl of MCF7 cell suspension (10^4 per ml, measured with haemocytometer) to 1 ml whole blood, giving ideally 100 MCF7 cells per ml whole blood (accurate values were determined using MIC in each case). The spiked blood was incubated with 200 μl anti-EpCAM functionalised magnetic microbeads (50 nm diameter, Miltenyi Biotec) with 100 μl FcR blocking reagent (Miltenyi Biotec) for 30 min on a roller at room temperature followed by erythrocytes lysis. A MACS column (MS, Miltenyi Biotec) was primed with 3 ml filtered running buffer. The blood lysate was allowed to flow under gravity through the column and the negative fraction containing only leukocytes was discarded. After removing the magnet, the magnetically labelled cells were eluted from the column using 1 ml filtered elution buffer (Miltenyi Biotec). Cells were eluted by pushing a plunger into the top of the column displacing fluid trapped in the mesh so that the positive fraction volume was slightly higher than the 1 ml of elution buffer; between 1.32 ml and 1.35 ml. For a control, the same procedure was repeated without the MCF7 cells. The protocol was repeated for five different blood donors.

III. RESULTS

A. Characterising the dielectric properties of MCF7 cells

Fig. 2 shows impedance scatter plots for a suspension of MCF7 cells mixed with 6 μm diameter polystyrene beads, which are used as reference particles. The x-axis is the cube root of the low frequency electrical impedance (proportional to cell diameter). The y-axis is the ratio of high to low frequency impedance—termed opacity. This parameter varies approximately inversely with the cell membrane capacitance. The size and opacity data are normalised with respect to the mean of the beads, which have a tight distribution, known size (6 μm diameter) and frequency independent dielectric properties. The beads are distinguished from debris on the basis of the phase signal (not shown). Fig. 2(a) shows impedance scatter plots for MCF7 cells measured directly after passage and re-suspension into PBS. A single population is observed that is well separated from the debris (cell fragments). The electrical impedance at low frequencies (below the relaxation of the membrane) accurately measures cell size.[22] Therefore, using the beads as reference particles, the diameter of the MCF7 cells can be estimated as 17.3 ± 1.9 μm ($\mu \pm \sigma$), similar to values reported elsewhere (18.2 μm).[6] An accurate determination of the membrane capacitance of the MCF7 cells can only be made by fitting impedance data over at least two decades of frequency (up to 100 MHz), which is currently not possible with the limited bandwidth of our electronics. Simulations (see below) indicate that the membrane capacitance is around 18 mF/m^2, which is in line with the literature and significantly greater than leukocytes (10–15 mF/m^2).

Fig. 2(b) shows impedance data for MCF7 cells that have been re-suspended in PBS for 2 h at room temperature. Immediately prior to measurement, the cells were labelled with both EpCAM-FITC and Propidium Iodide (PI) and the fluorescence from the cells measured simultaneously with impedance. The PI binds to DNA in the cells and is excluded from viable cells. Cells undergoing necrosis or late apoptosis have permeable membranes that allow the PI to enter the cell and nuclear membrane, and intercalate into the DNA causing thus rendering the cells fluorescent.

Fig. 2(b) shows that these cells have a broader distribution in size and in opacity than freshly harvested cells. The size and opacity of the main population is unchanged, but the distribution is skewed towards higher opacity and lower size. The figure also shows that the

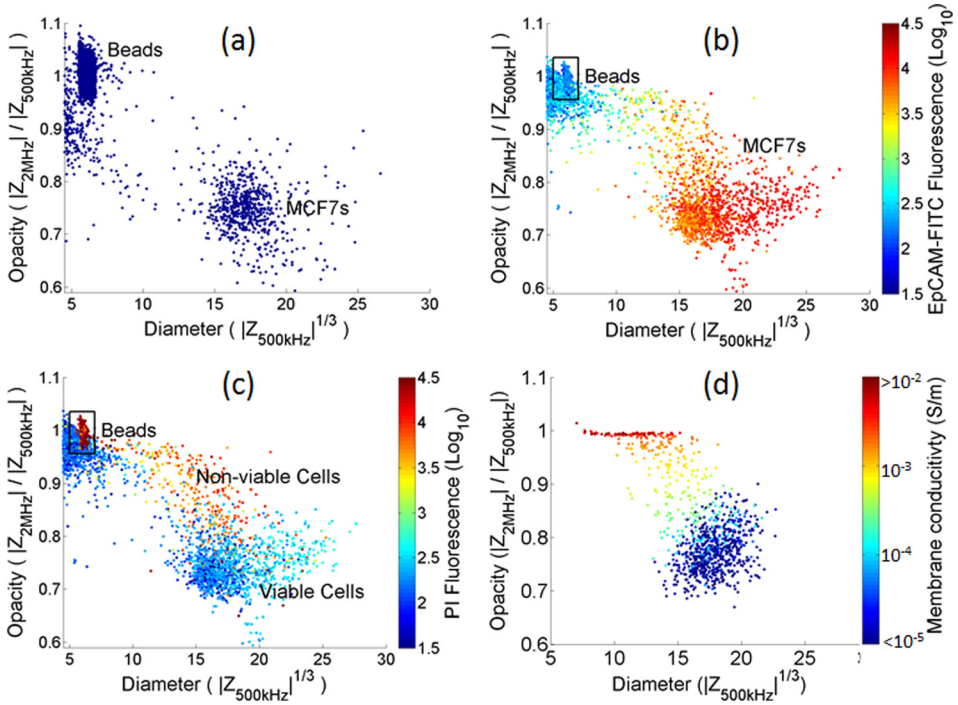

FIG. 2. Scatterplots of the impedance data plotted as opacity (Z at 2 MHz/Z at 0.5 MHz) vs diameter ($_3\sqrt{}$Z at 0.5 MHz). (a) Mixture of freshly harvested MCF7s and 6 μm diameter beads (10000 events). (b) and (c) mixture containing MCF7s suspended in PBS at room temperature for 2 h and 6 μm diameter beads (10000 events) colour coded for (b) EpCAM fluorescence and (c) PI fluorescence. (d) A simulated population of 1000 MCF7 cells, each with a different membrane conductivity in the range 10^{-8}–10^{-2} S/m. The cells were simulated using the following parameters: suspending medium ($\varepsilon = 80$ and $\sigma = 1.6$ S/m), membrane ($\varepsilon = 10$, $\sigma = 10^{-8}$–10^{-2} S/m, and thickness = 5 nm), cytoplasm ($\varepsilon = 60$ and $\sigma = 0.5$ S/m), nuclear envelope ($\varepsilon = 20$, $\sigma = 8\times10^{-3}$S/m, and d = 40 nm), and nucleoplasm ($\varepsilon = 80$ and $\sigma = 2$ S/m) (see the supplementary material).[32]

amount of EpCAM expression correlates with cell volume. Fig. 2(c) indicates that the main population of cells with high EpCAM expression has very little PI fluorescence. However, there is a sub-population of cells with high opacity, high PI fluorescence, and low EpCAM expression. These have highly permeable membranes and are also probably shedding membrane material after being kept for extended periods of time in suspension.[8] Note that the beads are fluorescent in the red channel and can be distinguished from the debris.

The cell membrane is an excellent electrical insulator[23–26] and at low frequencies cells behave as insulating particles. At higher frequencies (beyond the relaxation time of the membrane), the membrane becomes electrically transparent allowing the intracellular properties to be probed. However, non-viable cell has permeable membranes so that the impedance at both measurement frequencies (0.5 MHz and 2 MHz) will be the same, and governed by the intracellular properties. Broad-band dielectric measurement of cells in suspension show that the nucleus can be modelled as a sphere with a moderately insulating envelope ($\sigma \sim 10^{-3}$ S/m[24,27,28]). Non-viable cells therefore appear as small particles whose electrical size is determined by the properties of the nucleus—a trend that is apparent in Fig. 2(c).

The impedance properties of the cells were simulated using Maxwell's mixture theory[29] including the double-shell model that takes into account the properties of the nucleus.[27,30] Fig. 2(d) is a scatter plot of the simulated impedance for a population of 1000 MCF7 cells, calculated at 0.5 MHz and 2 MHz. The dielectric properties of the cytoplasm and nucleus were set to literature values[6,24,28,31] with a cell membrane capacitance of 18 mF/m^2 and radius = 9 μm. The main population (blue) gives a good fit to the measured data (Fig. 2(a)) and are in line with values determined by DEP cross over methods.[6] The scatter in the impedance data was

simulated by including a normal distribution (CV S.D. = 10%) in cell radius and each dielectric property (see the supplementary material[32]).

To model the effect of cell viability on impedance, the simulation also includes a variation in the membrane conductivity. This was varied in the range 10^{-8}S/m–10^{-2} S/m (on a log scale), simultaneously reducing the cell radius (on a linear scale from 9 μm to 6 μm) to mimic the changes observed due to cytoplasm shedding,[8] keeping the size of the nucleus unchanged. The simulation of Fig. 2(d) mirrors the experimental data of Fig. 2(c), with the most significant change due to the membrane conductivity in the range 10^{-4} S/m–10^{-3} S/m. This trend is consistent with theoretical predictions,[25] which shows that a membrane conductivity smaller than 10^{-5} S/m has little influence on the impedance data, whilst for conductivities greater than 10^{-2} S/m, the cell dielectric properties are governed by the internal properties, which in turn is dominated by the nucleus.

B. CTCs in whole blood

Analysis of CTCs in whole blood commonly requires some pre-processing to remove the abundant erythrocytes, for example, by lysis. Therefore, the electrical properties of MCF7 cells spiked into whole blood were measured after erythrocyte lysis. A 10 μl stock solution of MCF7 cells (5×10^6 /ml) was added to a 50 μl aliquot of whole blood and the MCF7 cells labelled by addition of 50 μl anti-EpCAM-FITC to the blood, followed by incubation for 10 min at 5 °C. The erythrocytes were then lysed as described above. The suspension was divided in half, one tube was analysed using MIC and the other by conventional flow cytometry (BD FacsAria).

Fig. 3 shows conventional flow cytometer (a) and MIC (b) scatter plots for MCF7 cells in lysed whole blood. The impedance data demonstrate clearer discrimination than the optical scatter (side scattered light (SSC) vs forward scattered (FSC)) data. For the FSC data, the mean of MCF7 population is 2σ from the mean of the leukocytes (where σ is the standard deviation of the MCF7 population). By comparison, the impedance data ($\sqrt[3]{|\mathbf{Z}_{500\text{kHz}}|}$) has a separation of 8σ. Impedance directly measures cell volume whereas the small angle scatter is a non-linear function of cell size. Fig. 3(b) also shows a small number of non-viable cells with high opacity as seen in Fig. 2(c). The low opacity of the MCF7 population compared to the leukocytes population is in line with the known higher membrane capacitance of the MCF7 cells.

The effect of the lysis chemistry on the MCF7 cells was also investigated. An aliquot of MCF7 cells was spiked into a suspension of leukocytes prepared by chemical lysis of whole blood and a second aliquot added to the same volume of whole blood which was mixed and then lysed as above. The impedance scatter plot (Fig. S1 in the supplementary material[32]) for the two samples (i.e., MCF7 cells exposed or not exposed to the lysis chemistry) shows that the cell properties are unaltered. Loss of cells after lysis was also estimated using impedance. Blood from three different donors was processed (each in triplicate) and the number of spiked

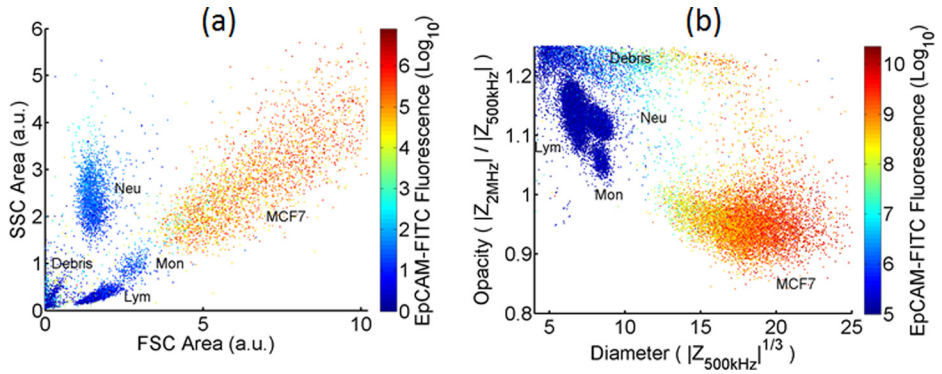

FIG. 3. Scatterplot of a mixture of leukocytes and MCF7 cells measured on (a) BD FacsAria and (b) Impedance cytometer (30 000 events in both cases). There is a greater separation between the electrical properties of the MCF7s and leukocytes in (b) compared with the optical properties (a).

MCF7 cells determined by impedance in each case. To ensure that the MCF7 cells and leukocytes could be counted using the same gate, each sample was analysed by normalising the data to the neutrophil populations. The CV of this normalising factor for the nine experiments was 6% for cell radius and 2% for opacity, indicating that the cell size and membrane capacitance remained unchanged. Furthermore, there was no significant difference in the ratio of the MCF7 to leukocyte count (Fig. S2 in the supplementary material[32]) if cells were spiked before or after lysis ($P = 0.997$, two tailed t-test). This demonstrates that the erythrocyte lysis protocol does not affect the MCF7 count cell or their electrical properties.

C. Enumeration limits

The detection and isolation of very small numbers of CTCs in large volumes of blood remains a challenge, particularly for non-immunological methods. In this work, we used impedance analysis to estimate the limit of detection of MCF7 cells spiked into whole blood following serial dilution. The optimum frequency for discriminating MCF7 from leukocyte was determined by measuring the impedance over a range of frequencies, and the optimum value was found to be approximately 4 MHz. Thus, all further experiments were performed at 0.5 MHz and 4 MHz.

MCF7 cells were added to whole blood from three suspensions of 3×10^6 cells/ml (measured with a haemocytometer), 1:10 dilution (3×10^5 cells/ml), and 1:100 dilution (3×10^4 cells/ml). In triplicate, 10 μl aliquots of each dilution was added to 50 μl aliquots of whole blood to give an approximate MCF7 to leukocyte ratio of 1:10, 1:100, and 1:1000. Erythrocytes were lysed and each sample was measured for 2, 5, and 13 min, respectively, ensuring that at least 100 MCF7s were measured. In each case, a small known aliquot of 6 μm diameter reference beads was added so that identical enumeration gates could be applied to all samples. For control experiments, 10 μl of filtered cell culture media was added to 50 μl whole blood, and measured for 13 min after erythrocyte lysis. Each dilution experiment was performed in triplicate for three different blood donors and MCF7 stock solutions (27 different experiments plus 9 controls).

The impedance scatter results together with the enumeration gates (Fig. S3 in the supplementary material[32]) show that the MCF7 cells can easily be distinguished from the leukocytes at very low ratios (1:1000). Out of the nine control experiments, five had zero MCF7 cells in the gate. In the remaining four samples, either one or two events were detected. The results are summarised in Fig. 4, which shows the experimentally measured ratios of leukocytes to MCF7 cells for each blood sample and each dilution. The actual ratios of MCF7 cells to leukocytes depend on the absolute leukocyte count in each blood sample. The nominal ratios of MCF7 to leukocyte (1:10, 1:100, and 1: 1000) were based on an estimated mean leukocyte count of 6×10^6 cells/ml but as shown in Fig. 4, the experimental ratios were slightly higher.

D. Cell pre-enrichment

The impedance cytometer enumerates every single cell passing through the measurement volume, but analysis of whole blood at 5×10^9 erythrocytes/ml would take a very long time. Chemical lysis removes nearly all the erythrocytes, leaving in the region of $4–11 \times 10^6$ leukocytes per ml. The cell suspension must be diluted to minimise coincidence, and typically, 1 ml of blood is diluted to 18.3 ml by the lysis protocol. At a volumetric throughput of 40 μl/min, this would still take 7.6 h to process. Therefore, analysis of very low abundance cells (CTCs are typically 1 per 10^6 leukocytes) by impedance cytometry requires pre-concentration of cells.

Pre-enrichment of MCF7 cells was carried out as described in Sec. II D. To each pre-enriched sample 6 μm diameter beads were added prior to measurement by MIC; data were normalised against the beads so that the same enumeration gates (Fig. S3 in the supplementary material[32]) could be used in all experiments. The average MCF7 count in the 10 μl stock was determined from MIC measurements of an 80 μl aliquot. The positive fractions from the MACS column containing the concentrated MCF7 cells were measured for 15 min, during which approximately half of the volume was measured. The expected MCF7 count should therefore

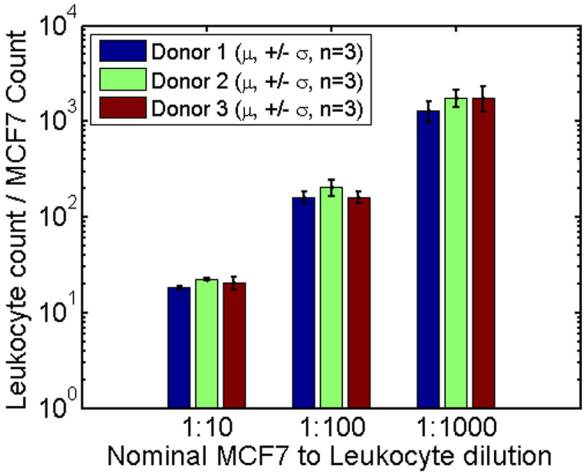

FIG. 4. Bar chart showing the ratios of leukocytes to MCF7 cells for different nominal spiking ratios. Blood from three separate donors was measured and experiments were performed in triplicate. For control experiments (which followed an identical protocol, without MCF7) 0 events were seen within the MCF7 gate in five cases, 1 event in 3 cases and 3 events in 1 case. Around 100 MCF7 cells were measured in the 1:1000 dilution samples. The nominal ratio is based on a nominal leukocyte count of 6 cells/nL. Actual measured samples had higher leukocyte counts thus increasing the measured leukocyte to MCF7 ratios.

be equal to the number of MCF7s spiked into whole blood multiplied by the ratio of measured to eluted volume.

Impedance scatterplots of the positive fraction for the spiked sample and control sample are shown in Fig. 5. Table I summarises the data. For three out of five samples, the number of MCF7 cells closely matches the expected numbers (samples 2, 4, and 5). In sample 1, the number of measured MCF7s was significantly lower than expected. In sample 3, MCF7s were higher by ∼30%, yet no cells were found in the corresponding control sample. These results indicate that positive antibody selection of MCF7 cells at very low concentrations (100 per ml blood) using a simple MACS protocol recovers a large percentage of the original population. Furthermore, virtually no positive events were seen in the control experiments (typically 1 or zero).

In summary, 1 ml of whole blood is spiked with approximately 100 MCF7 cells. The entire sample is incubated with EpCAM magnetic beads, then lysed and diluted into a volume of 18.3 ml. This is passed through a MACS column, the eluate discarded and the magnetically labelled cells recovered into a volume of 1.35 ml, of which 50% is measured. Both MCF7 cells and contaminating leukocytes are identified and enumerated based on their unique impedance signals. The mean recovery of MCF7 cells was $92\% \pm 34\%$ ($n = 5$). The number of

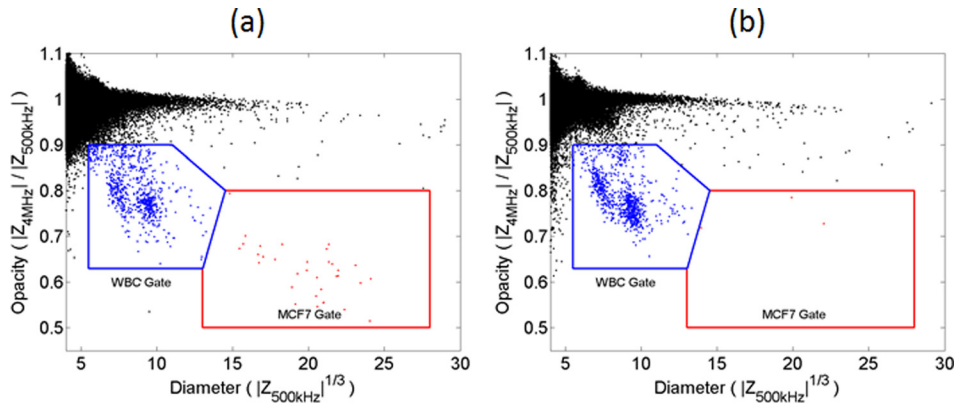

FIG. 5. Impedance scatterplot for a sample of the positive fraction of whole lysed blood after MACS enrichment (donor no.2). In (a), an estimated 74 MCF7s were spiked into 1 ml of whole blood. (b) shows the control experiment where no MCF7 cells were added. This scatter has the maximum number of events in the MCF7 gate for the control experiments—3 in this case.

TABLE I. Results of EpCAM enrichment of approximately 100 MCF7s spiked into 1 ml whole blood.

	MCF7 events		MCF7 events (Control)	
Blood donor sample nos.	Expected	Measured	Expected	Measured
1	30	11	0	0
2	32	33	0	3
3	34	45	0	1
4	33	32	0	1
5	24	22	0	0

contaminating leukocytes in the positive fractions (see gate in Fig. 5) was $1\,130 \pm 695$ (in 50% of the sample). This corresponds to a log 3.5 depletion.

Many different techniques have been developed for CTC isolation. While the capture efficiency for spiked cells can approach 100%, achieving a highly pure, leukocyte free CTC fraction remains a challenge. Ozkumur *et al.*[33] have recently developed a continuous flow microfluidic sorter which utilised deterministic lateral displacement (DLD) to first remove erythrocytes and platelets, followed by inertial focusing and magnetic separation to separate tumour cells from whole blood. In positive enrichment mode, where cells were sorted based on EpCAM marker, the capture efficiency was between 77.8% and 98.6% (depending on the level of EpCAM expression of the tumour cell line used). On average, a background of 1500 leukocytes per ml of whole blood was observed in this positive selection mode. When operating in negative selection mode (CD45 depletion) for antibody-independent tumour selection, there was a higher level of leukocyte contamination (average of 32 000 leukocytes per ml). The negative-selection protocol was later improved by utilising both CD45 and CD66b antibodies,[34] achieving an average 3.8-log depletion (1100 contaminating leukocytes per ml). Other CTC isolation methods include capture onto surfaces such as microfabricated posts within microfluidic devices.[35] These technologies have demonstrated very high purity capture, but require analysis of cells *in-situ*.

While it was shown many years ago that DEP could separate unlabelled tumour cells from blood based on their dielectric properties,[5] devices have only recently been developed to process the large numbers of cells found in a 7.5 ml blood sample. Gupta *et al.*[9] used continuous flow DEP-FFF to capture on average 75% of tumour cells spiked into peripheral blood mononuclear cells (PBMCs) isolated from a 7.5 ml blood sample. The percentage reduction in PBMCs was 99.33%, leaving 11 000 PMBCs per ml of blood after processing. Using similar technology, Shim *et al.*[10] achieved similar capture efficiencies for spiked cells. Additionally, CTCs were captured from clinical samples for further molecular analysis, demonstrating that captured CTCs had the KRAS G13D mutation. The capture purity was lower than expected from the statistical differences in dielectric properties between blood and tumour cells, and Gascoyne and Shim[4] postulated that this was due to contamination by senescent PBMCs. A second DEP stage was used to increase the capture purity of spiked cells to 20%. All of these technologies enable recovery of CTCs into a small volume for further analysis.

The concentration of spiked cells used in our experiments is within the upper range of cell numbers found in clinical samples.[36] Nevertheless, the combination of a simple MACS separation protocol with label-free impedance analysis demonstrates high efficiency enumeration of spiked cells, with a 3.5 log increase in purity from a 1 ml blood sample. Furthermore, the large difference in the impedance properties of the MCF7 cells from whole blood provides a clear and simple method for label-free identification of these cells, which should be applicable across a wide spectrum of tumour cells, e.g., the NCI-60 panel, all of which have similar dielectric properties.[6]

IV. CONCLUSIONS

Single cell microfluidic impedance cytometry was used to examine the dielectric properties of a mixture of immortalised breast cancer cells and human leukocytes. The large size and

membrane capacitance of these cells (in common with most tumour cells) give rise to very clear discrimination from leukocytes on an impedance scatter plot. Whole blood containing low levels of MCF7 cells was processed to remove erythrocytes using a saponin/formic acid lysis protocol, which reduced the background cell count by approximately 3 orders of magnitude. This lysis protocol had no influence on the MCF7 count ($p > 0.997$), neither did it alter the dielectric properties. Impedance cytometry was used to enumerate low numbers of MCF7s (1:1000 leukocytes) spiked into whole blood and the method is only limited by the volumetric throughput of the cytometer. To detect very low, clinically relevant numbers of MCF7s, a simple MACS protocol was used to pre-enrich EpCAM positive cells before MIC measurement. Following MACS enrichment, it was possible to detect approximately 100 MCF7s spiked into 1 ml whole blood with a recovery rate close to 100%. The MACS protocol achieved a log 3.5 depletion of leukocytes which compares favorably with other CTC isolation methods. Control experiments using 1 ml blood without MCF7s showed virtually zero events in the same gate. This work demonstrates the potential for an in-line, high throughput label-free cell identification, and enumeration method with novel microfluidic cell isolation technologies. For example, a combination of label-free pre-enrichment techniques, such as dielectrophoresis,[10] with impedance based cell identification and enumeration together with further single cell sorting could provide pure populations of rare cells like CTCs.

ACKNOWLEDGMENTS

The authors acknowledge the Technology Strategy Board and EPSRC (TS/G001405/1) for funding this work. H.M. would like to acknowledge the Royal Society for funding. We thank Katie Chamberlain for fabricating the chips and Judith Holloway for useful discussions.

[1]Y. C. Ma, L. Wang, and F. L. Yu, "Recent advances and prospects in the isolation by size of epithelial tumor cells (ISET) methodology," Technol. Cancer Res. Treat. **12**, 295–309 (2013).
[2]J. M. Park, J. Y. Lee, J. G. Lee, H. Jeong, J. M. Oh, Y. J. Kim, D. Park, M. S. Kim, H. J. Lee, J. H. Oh, S. S. Lee, W. Y. Lee, and N. Huh, "Highly efficient assay of circulating tumor cells by selective sedimentation with a density gradient medium and microfiltration from whole blood," Anal. Chem. **84**, 7400–7407 (2012).
[3]S. C. Hur, N. K. Henderson-MacLennan, E. R. McCabe, and D. di Carlo, "Deformability-based cell classification and enrichment using inertial microfluidics," Lab Chip **11**, 912–920 (2011).
[4]P. R. C. Gascoyne and S. Shim, "Isolation of circulating tumor cells by dielectrophoresis," Cancers **6**, 545–579 (2014).
[5]F. F. Becker, X. B. Wang, Y. Huang, R. Pethig, J. Vykoukal, and P. R. C. Gascoyne, "Cell biology separation of human breast cancer cells from blood by differential dielectric affinity," Proc. Natl. Acad. Sci. U.S.A. **92**, 860–864 (1995).
[6]P. R. C. Gascoyne, S. Shim, J. Noshari, F. F. Becker, and K. Stemke-Hale, "Correlations between the dielectric properties and exterior morphology of cells revealed by dielectrophoretic field-flow fractionation," Electrophoresis **34**, 1042–1050 (2013).
[7]R. Pethig, "Review article-dielectrophoresis: Status of the theory, technology, and applications," Biomicrofluidics **4**, 022811 (2010).
[8]S. Shim, P. R. C. Gascoyne, J. Noshari, and S. Stemke-Hale, "Dynamic physical properties of dissociated tumor cells revealed by dielectrophoretic field-flow fractionation," Integr. Biol. **3**, 850–862 (2011).
[9]V. Gupta, I. Jafferji, M. Garza, V. O. Melnikova, D. K. Hasegawa, R. Pethig, and D. W. Davis, "ApoStream(™), a new dielectrophoretic device for antibody independent isolation and recovery of viable cancer cells from blood," Biomicrofluidics **6**, 24133 (2012).
[10]S. Shim, K. Stemke-Hale, A. M. Tsimberidou, J. Noshari, T. E. Anderson, and P. R. C. Gascoyne, "Antibody-independent isolation of circulating tumor cells by continuous-flow dielectrophoresis," Biomicrofluidics **7**, 011807 (2013).
[11]J. Voldman, "Electrical forces for microscale cell manipulation," Annu. Rev. Biomed. Eng. **8**, 425–454 (2006).
[12]R. Pethig, V. Bressler, C. Carswell-Crumpton, Y. Chen, L. Foster-Haje, M. E. García-Ojeda, R. S. Lee, G. M. Lock, M. S. Talary, and K. M. Tate, "Dielectrophoretic studies of the activation of human T lymphocytes using a newly developed cell profiling system," Electrophoresis **23**, 2057–2063 (2002).
[13]H. W. Su, J. L. Prieto, and J. Voldman, "Rapid dielectrophoretic characterization of single cells using the dielectrophoretic spring," Lab Chip **13**, 4109–4117 (2013).
[14]H. Morgan, T. Sun, D. Holmes, S. Gawad, and N. G. Green, "Single cell dielectric spectroscopy," J. Phys. D: Appl. Phys. **40**, 61–70 (2007).
[15]T. Sun and H. Morgan, "Single-cell microfluidic impedance cytometry: A review," Microfluid. Nanofluid. **8**(4), 423–443 (2010).
[16]D. Holmes, D. Pettigrew, C. H. Reccius, J. D. Gwyer, C. V. Berkel, J. Holloway, D. E. Davie, and H. Morgan, "Leukocyte analysis and differentiation using high speed microfluidic single cell impedance cytometry," Lab Chip **9**, 2881–2889 (2009).
[17]X. Han, C. van Berkel, J. Gwyer, L. Capretto, and H. Morgan, "Microfluidic lysis of human blood for leukocyte analysis using single cell impedance cytometry," Anal. Chem. **84**, 1070–1075 (2012).
[18]H. Song, Y. Wang, J. M. Rosano, B. Prabhakarpandian, C. Garson, K. Panta, and E. A. Lai, "A microfluidic impedance flow cytometer for identification of differentiation state of stem cells," Lab Chip **13**, 2300–2310 (2013).

[19]C. Küttel, E. Nascimento, N. Demierre, T. Silva, T. Braschler, P. H. Renaud, and A. G. Oliva, "Label-free detection of Babesia bovis infected red blood cells using impedance spectroscopy on a microfabricated flow cytometer," Acta Trop. **102**, 63–68 (2007).
[20]H. Choi, K. B. Kim, C. S. Jeon, I. Hwang, S. Lee, H. K. Kim, H. C. Kim, and T. D. Chung, "A label-free DC impedance-based microcytometer for circulating rare cancer cell counting," Lab Chip **13**, 970–977 (2013).
[21]D. Spencer and H. Morgan, "Positional dependence of particles in microfluidic impedance cytometry," Lab Chip **11**, 1234–1239 (2011).
[22]D. Spencer, G. Elliott, and H. Morgan, "A sheath-less combined optical and impedance micro-cytometer," Lab Chip **14**, 3064–3073 (2014).
[23]K. Asami, Y. Takahashi, and S. Takashima, "Frequency domain analysis of membrane capacitance of cultured cells (HeLa and myeloma) using the micropipette technique," Biophys. J. **58**, 143–148 (1990).
[24]Y. Polevaya, I. Ermolina, M. Schlesinger, B. Z. Ginzburg, and Y. Feldman, "Time domain dielectric spectroscopy study of human cells: II. Normal and malignant white blood cells," Biochim. Biophys. Acta **1419**, 257–271 (1999).
[25]A. Di. Biasio and C. Cametti, "On the dielectric relaxation of biological cell suspensions: The effect of the membrane electrical conductivity," Colloids Surf., B **84**, 433–441 (2011).
[26]U. Lei, P.-H. Sun, and R. Pethig, "Refinement of the theory for extracting cell dielectric properties from dielectrophoresis and electrorotation experiments," Biomicrofluidics **5**, 044109 (2011).
[27]A. Irimajiri, T. Hanai, and A. Inouye, "A dielectric theory of 'multi-stratified shell' model with its application to a lymphoma cell," J. Theor. Biol. **78**, 251–269 (1979).
[28]A. C. Sabuncu, J. Zhuang, J. F. Kolb, and A. Beskok, "Microfluidic impedance spectroscopy as a tool for quantitative biology and biotechnology," Biomicrofluidics **6**, 034103 (2012).
[29]T. Sun, C. Bernabini, and H. Morgan, "Single-colloidal particle impedance spectroscopy: Complete equivalent circuit analysis of polyelectrolyte microcapsules," Langmuir **26**(6), 3821–3828 (2009).ôôôô
[30]T. B. Jones, *Electromechanics of Particles* (Cambridge University Press, Cambridge, UK, 1995).
[31]A. Irimajiri, Y. Doida, T. Hanai, and A. Inouye, "Passive electrical properties of cultured murine lymphoblast (L5178Y) with reference to its cytoplasmics membrane, nuclear envelope and intracellular phases," J. Membr. Biol. **38**, 209–232 (1978).
[32]See supplementary material at http://dx.doi.org/10.1063/1.4904405 for additional figures. (S1) example scatterplots of the impedance data for MCF7s spiked into blood before or after lysis. (S2) numerical comparison between spiking MCF7 cells into whole blood before and after lysis. (S3) Example scatterplots of the impedance of mixture of leukocytes and MCF7 cells at different concentrations. (S4) Parameters used in the double shell model simulation of Fig. 2(d).
[33]E. Ozkumur, A. M. Shah, J. C. Ciciliano, B. L. Emmink, D. T. Miyamoto, E. Brachtel, M. Yu, P. Chen, B. Morgan, J. Trautwein, A. Kimura, S. Sengupta, S. L. Stott, N. M. Karabacak, T. A. Barber, J. R. Walsh, K. Smith, P. S. Spuhler, J. P. Sullivan, R. J. Lee, D. T. Ting, X. Luo, A. T. Shaw, A. Bardia, L. V. Sequist, D. N. Louis, S. Maheswaran, R. Kapur, D. A. Haber, and M. Toner, "Inertial focusing for tumor antigen-dependent and independent sorting of rare circulating tumor cells," Sci. Transl. Med. **5**, 179ra47 (2013).
[34]N. M. Karabacak, P. S. Spuhler, F. Fachin, E. J. Lim, V. Pai, E. Ozkumur, J. M. Martel, N. Kojic, K. Smith, P. Chen, J. Yang, H. Hwang, B. Morgan, J. Trautwein, T. A. Barber, S. L. Stott, S. Maheswaran, R. Kapur, D. A. Haber, and T. Mehmet, "Microfluidic, marker-free isolation of circulating tumor cells from blood samples," Nat. Protoc. **9**, 694–710 (2014).
[35]B. J. Kirby, M. Jodari, M. S. Loftus, G. Gakhar, E. D. Pratt, C. Chantal-Vos, J. P. Gleghorn, S. M. Santana, H. Liu, J. P. Smith, V. N. Navarro, S. T. Tagawa, N. H. Bander, D. M. Nanus, and P. Giannakakou, "Functional characterization of circulating tumor cells with a prostate-cancer-specific microfluidic device," PLoS ONE **7**(4), e35976 (2012).
[36]M. Cristofanilli, G. T. Budd, M. J. Ellis, A. Stopeck, J. Matera, M. C. Miller, J. M. Reuben, G. V. Doyle, W. J. Allard, L. Terstappen, and D. F. Hayes, "Circulating tumor cells, disease progression, and survival in metastatic breast cancer," N. Engl. J. Med. **351**, 781–791 (2004).